

The effect of phonon confinement on perpendicular electron transport in a GaAs/GaAlAs superlattice

This article has been downloaded from IOPscience. Please scroll down to see the full text article.

1990 J. Phys.: Condens. Matter 2 119

(<http://iopscience.iop.org/0953-8984/2/1/009>)

View [the table of contents for this issue](#), or go to the [journal homepage](#) for more

Download details:

IP Address: 171.66.16.96

The article was downloaded on 10/05/2010 at 21:22

Please note that [terms and conditions apply](#).

The effect of phonon confinement on perpendicular electron transport in a GaAs/GaAlAs superlattice

I Dharssi and P N Butcher

Department of Physics, University of Warwick, Coventry, UK

Received 29 August 1989

Abstract. Recent experimental and theoretical results indicate that optical phonons in a GaAs/Ga_{1-x}Al_xAs heterojunctions show strong spatial modulation. The form of the modulation has been controversial. However, it has recently been shown that the scalar potential of the electric field associated with the phonons is well described by the dielectric continuum model. We present the results of the first calculation of electron mobility in a GaAs/Ga_{1-x}Al_xAs superlattice which takes into account the confinement of both electrons and optical phonons. The electron mobility for a low-density non-degenerate electron gas is evaluated by iterative numerical solution of the linearised Boltzmann equation. The modulation of the phonons reduces the scattering to 50% of that predicted using bulk phonons and the predicted mobility is significantly increased.

1. Introduction

The novel features of a superlattice (narrow miniband width, highly anisotropic band structure and much reduced Brillouin zone width in the growth direction) have led to a great deal of interest in their properties. Electron transport perpendicular to the superlattice layers has been the subject of many experimental and theoretical studies. In polar semiconductors at room temperature electron-LO phonon scattering is the dominant scattering mechanism. This is also assumed to be true for superlattices made of polar semiconductor materials. Several authors have shown that the form of the optic lattice vibrations of superlattices strongly deviates from that in the corresponding bulk materials. The effect of this on scattering rates have been calculated [1–4]. However, previous calculations of electron mobilities in superlattices have assumed bulk phonons [5, 6].

In this paper the effect of the superlattice structure on both electrons and optical phonons is taken fully into account in a lattice matched GaAs/Ga_{1-x}Al_xAs superlattice at 300 K subjected to a small electric field in the direction perpendicular to the layers. Experimental studies have shown evidence of Bloch conduction in this system [7, 8]. We therefore use the Boltzmann transport equation to calculate electron mobilities in the superlattice growth direction with polar optical phonon scattering taken as dominant. Attention is focused on low doping levels so that screening and inter-band scattering can be neglected.

2. Electrons

Effective mass theory is used to calculate the miniband structure and envelope function

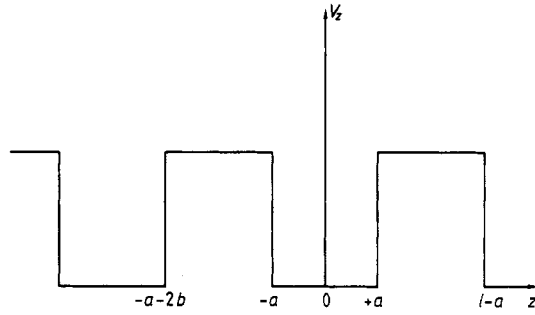


Figure 1. The Kronig-Penney potential.

of the electron states. For simplicity the small difference in effective mass between the GaAs and $\text{Ga}_{1-x}\text{Al}_x\text{As}$ layers is ignored. The superlattice potential is of the Kronig-Penney type with the same periodicity as the superlattice (see figure 1). In the manner of Warren *et al* and Palmier *et al* [5, 6] the miniband dispersion is represented by the phenomenological form

$$\varepsilon_k = (\hbar^2 k_{\parallel}^2 / 2m^*) + \Delta(1 - \cos k_z l) \quad (1)$$

where 2Δ is the miniband width obtained from the Kronig-Penney model. The barrier height is taken to be 250 meV which corresponds to an Al concentration in the $\text{Al}_x\text{Ga}_{1-x}\text{As}$ layer of $x = 0.3$ [27].

The envelope function is written in the tight binding formalism as:

$$\Psi_k = \sqrt{l/V} \exp(ik_{\parallel} \cdot \mathbf{x}_{\parallel}) \sum_{n=-N/2}^{n=+N/2} \phi(z - nl) \exp(ik_z nl) \quad (2)$$

where $\mathbf{k}_{\parallel} = k_x \hat{i} + k_y \hat{j}$, $\mathbf{x}_{\parallel} = x \hat{i} + y \hat{j}$ and $\phi(z)$ is the normalised eigenfunction of the Hamiltonian for a single potential well of width $2a$ and barrier height 250 meV centred at $z = 0$. The normalisation constant in (2) is determined for the case when the overlap of adjacent ϕ s is ignored so that

$$\phi(z - nl)\phi(z - ml) = \delta_{n,m} \phi^2(z - nl) \quad (3)$$

3. Scalar potential of the optic phonon modes

The optic vibrational modes of thin layer structures are known to deviate strongly from those of the corresponding bulk modes [9]. This has been the subject of much investigation [10–18]. Until recently, however, most studies have used macroscopic models or linear chain models. The difficulty with macroscopic models is that no unambiguous formulation of the boundary conditions exists. While, simple linear chain models do not take proper account of the Coulomb interaction and are only applicable when the phonon wave vector is in the growth direction.

The validity of these models remains in doubt and their predictions are often quite different. In particular there has been controversy over the form of guided modes in heterostructures. The dielectric continuum model (DCM) predicts the vibrational modes to have antinodes in U_z (the optical displacement in the superlattice growth direction) at the interfaces and nodes in the scalar potential [16–18]. However, other models predict that guided modes have nodes in U_z at the interface and anti-nodes in the scalar potential [10–15]. More realistic microscopic models have appeared [19–24]. They are

heavily numerical and intractable for transport calculations. Recently, however, a comparison of the DCM with one such microscopic model of the superlattice has been reported [21]. This has shown that while the optical displacement of the ions is not well described by the DCM, in the limit of vanishing bulk phonon dispersion, the scalar potential for the two models are in good agreement for both guided and interface modes. Fortunately it is the scalar potential which is important for studies of scattering rates and transport. Some authors [4, 10] have imposed the conditions that $U_z = 0$ at the interfaces for guided modes. This leads to a scalar potential which has anti-modes at the interfaces and thus an incorrect treatment of electron scattering.

We have therefore used the DCM model to obtain the scalar potential associated with the normal modes of the superlattice phonons. In this model the Born and Huang phenomenological equations together with electrostatic boundary conditions are applied [25]. LO solutions are obtained when:

$$\kappa_i(\omega)\nabla^2 V(\mathbf{r}) = 0 \quad (4)$$

where $\kappa_i(\omega)$ is the frequency dependent dielectric constant in material i (with $i = 1$ for GaAs and $i = 2$ for $\text{Ga}_{1-x}\text{Al}_x\text{As}$) and $V(\mathbf{r})$ is the scalar potential of the electric field associated with the LO phonons. The superlattice periodicity implies that $V(\mathbf{r})$ must be of the form:

$$V_\lambda(\mathbf{r}) = \exp(i\mathbf{q}_\parallel \cdot \mathbf{x}_\parallel) f(z)$$

where

$$f(z + nl) = f(z) \exp(iQnl) \quad (5)$$

with l denoting the periodicity of superlattice (see figure 1) and λ being a mode label.

We find that the superlattice optic phonons are of two types: guided and interface modes. For guided modes $\kappa_i(\omega) = 0$ in one of the superlattice materials in which the normal modes are confined, e.g. when $\omega = \omega_{\text{LO}}^{\text{GaAs}}$, we write $f(z) = f_G(z)$ with

$$f_G(z) = \begin{cases} A_G \cos(m\pi z/2a), & m = 1, 3, 5, \dots \\ A_G \sin(m\pi z/2a), & m = 2, 4, 6, \dots \end{cases} \quad |z| < a \quad (\text{region 1}) \quad (6)$$

$$0 \quad -l + a < z < -a \quad (\text{region 2}).$$

Similarly, for interface modes $\nabla^2 V(\mathbf{r}) = 0$ and we write $f(z) = f_I(z)$ with

$$f_I(z) = \begin{cases} A_I \exp(q_\parallel z) + B_I \exp(q_\parallel z) & |z| < a \\ C_I \exp(q_\parallel z) + D_I \exp(q_\parallel z) & -l + a < z < -a. \end{cases} \quad (7)$$

In both cases the normal modes can be expressed in terms of a scalar potential $V_\lambda(\mathbf{r})$ by writing

$$W_\lambda(\mathbf{r}) = c_i(-\nabla V_\lambda(\mathbf{r})) \quad (8)$$

where c_i is material dependent and is given by the Born and Huang phenomenological equations [25]:

$$c_i(\omega_\lambda) = \omega_{\text{TO}_i} [\epsilon_0(\kappa_{0_i} - \kappa_{z_i})]^{1/2} [\rho_{r_i}(\omega_\lambda^2 - \omega_{\text{TO}_i}^2)]^{-1/2}. \quad (9)$$

When the normal modes are quantised (see [26] and the Appendix) we find that the scalar potential is given by

$$V(\mathbf{r}) = \sum_\lambda \left(\frac{\hbar}{2\omega_\lambda \rho_{r_i}} \right)^{1/2} (a_\lambda^\dagger + a_\lambda) f(z) \exp(i\mathbf{q}_\parallel \cdot \mathbf{x}_\parallel). \quad (10)$$

4. Scattering rates and transport theory

Having obtained the scalar potential we can now calculate the scattering rates by using Fermi's golden rule. The details are given in the Appendix with the following results. For guided modes:

$$T(\mathbf{k}, \mathbf{k}') = 2\pi \frac{l}{2a} \alpha \sum_m \left[(\mathbf{k}_{\parallel} - \mathbf{k}'_{\parallel})^2 + \left(\frac{m\pi}{2a} \right)^2 \right]^{-1} \left| \int_{-a}^{+a} \cos \frac{m\pi}{2a} \phi^2(z) dz \right|^2. \quad (11)$$

For interface modes:

$$\begin{aligned} T(\mathbf{k}, \mathbf{k}') &= \frac{\pi l \alpha}{4} \left[q_{\parallel} \left(\sinh(2q_{\parallel} a) + \left| \frac{D_1}{A_1} \right|^2 \exp(q_{\parallel} l) \sinh(2q_{\parallel} b) \frac{c_2^2(\omega_{\lambda})}{c_1^2(\omega_{\lambda})} \right) \right]^{-1} \\ &\times \left| \int_{-l/2}^{+l/2} \frac{f_1(z)}{A_1} \phi^2(z) \left(\frac{\rho_{r1}}{\rho_{r1}} \right)^{1/2} dz \right|^2 \frac{\omega_{\text{LO}}^{\text{GaAs}} c_1^2(\omega_{\text{LO}}^{\text{GaAs}})}{\omega_{\lambda} c_1^2(\omega_{\lambda})} \\ &\times \delta_{(k_{\parallel} - k'_{\parallel}), q} \delta_{(k_{\perp} - k'_{\perp}), Q} \end{aligned} \quad (12)$$

where

$$\alpha = \frac{e^2 \omega_{\text{LO}}^{\text{GaAs}}}{V \epsilon_0} \left(\frac{1}{\kappa_z^{\text{GaAs}}} - \frac{1}{\kappa_0^{\text{GaAs}}} \right) (n_{\lambda} + \frac{1}{2} \pm \frac{1}{2}) \delta(\epsilon_{k'} - \epsilon_k \pm \hbar \omega_{\lambda}).$$

The scattering rates given for intra-band scattering in the lowest miniband. Since we are assuming non-degenerate statistics inter-band scattering is not considered

If a small electric field is applied to the superlattice perpendicular to the layers, the electron distribution function can be written as

$$f = f_0 + g \quad (13)$$

where f_0 is the Fermi-Dirac distribution and g is the first order perturbation. From the linearised Boltzmann transport equation, assuming non-degenerate statistics, i.e., $f_0 \ll 1$, we have:

$$g(\mathbf{k}) = \tau(\mathbf{k}) \int g(\mathbf{k}') P(\mathbf{k}', \mathbf{k}) d^3 \mathbf{k}' + \frac{e}{\hbar} E_z \frac{df_0}{dk_z} \quad (14)$$

where $P(\mathbf{k}, \mathbf{k}') = (V/8\pi^3) T(\mathbf{k}, \mathbf{k}')$ and

$$\tau^{-1}(\mathbf{k}) = \int P(\mathbf{k}, \mathbf{k}') d^3 \mathbf{k}' \quad (15)$$

is the lifetime of electron state \mathbf{k} .

In calculating the lifetimes the scattering rates given in (11) and (12) are used. For guided modes only the odd- m modes contribute to intra-band scattering [1], and scattering rates decrease significantly as m increases, thus only the $m = 1$ mode is considered. However, the interface modes dominate the scattering. There are four interface modes and their frequencies approach the bulk optical frequencies of the constituent materials as $q \rightarrow 0$, (21). It is in this limit when scattering is largest. The two interface modes whose frequencies are near $\omega_{\text{TO}}^{\text{GaAs}}$ and $\omega_{\text{TO}}^{\text{AlGaAs}}$ hardly contribute to the scattering since $c_l(\omega_{\text{TO}}) \rightarrow \infty$. Scattering is due mainly to the mode whose frequency is near $\omega_{\text{LO}}^{\text{AlGaAs}}$. The scalar potential associated with this mode is approximately symmetric in the GaAs layer as $q \rightarrow 0$. The mode whose frequency is near $\omega_{\text{LO}}^{\text{GaAs}}$ has a scalar

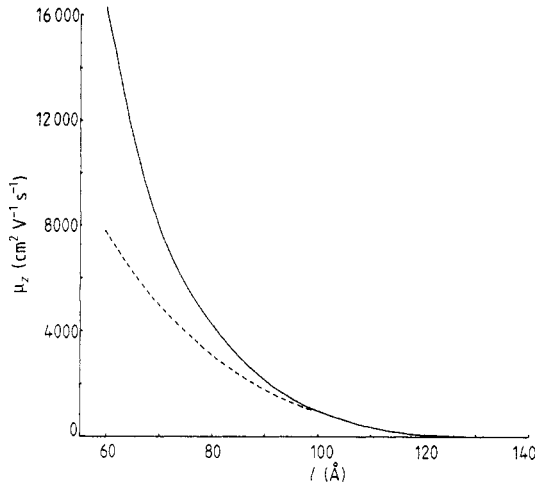


Figure 2. Mobility at 300 K as a function of superlattice periodic length. The superlattice material parameters are taken from [14]. Full curve: DCM; broken curve: bulk phonons.

potential which is approximately antisymmetric in the GaAs layer when $\mathbf{q} \rightarrow 0$, and therefore makes only a weak contribution to the scattering. For simplicity the weak dependence of the interface mode frequency ω_λ on the wavevector is ignored and we put $\omega_\lambda = \omega_{\text{LO}}^{\text{AlGaAs}} (= \omega_{\text{LO}}^{\text{GaAs}})$ for the symmetric (antisymmetric) modes respectively.

The first order perturbation in the electron distribution g is calculated from (14) using an iterative numerical technique [6]. From g the mobility perpendicular to the superlattice layers is easily calculated. The result is shown as a function of l when $a = b$ in figure 2. For comparison the mobility when bulk phonons are assumed is also shown.

5. Discussion

In this paper we have taken into account the effect of the superlattice structure on both electron and phonon properties. We see from figure 2 that this leads to a 50% reduction in the scattering rate. Due to the highly anisotropic superlattice miniband structure and the inelastic nature of electron-LO phonon scattering no relaxation time approximation exists. Hence an iterative scheme is used to derive the perturbed electron distribution function and calculate the electron mobility. The theory needs to be extended to allow for finite bulk phonon dispersion. This is particularly important for the GaAs/Ga_{0.7}Al_{0.3}As superlattice because the optic phonon branches of bulk GaAs and Ga_{0.7}Al_{0.3}As overlap. We note here that, even in frequency regions where the optical bulk branches overlap, confined modes still exist [23].

To compare our results with experiment more experimental data is needed. It may also be necessary to take account of other scattering mechanism besides LO phonon scattering. In particular scattering due to interface roughness may be important for superlattices with narrow layers [28]. We relegate these problems to another paper.

Appendix

Starting from (8) we write

$$W_\lambda(\mathbf{r}) = c_\lambda(\omega_\lambda)(i\mathbf{q}_\parallel f(z) + \hat{\mathbf{k}} \partial f / \partial z) \exp(i\mathbf{q}_\parallel \cdot \mathbf{x}_\parallel). \quad (16)$$

To ensure that $W_\lambda(\mathbf{r})$ is normalised to unity in the whole superlattice we impose the following condition on $f(z)$:

$$\int_{-l+a}^{+a} \left(|q_\parallel|^2 |f(z)|^2 + \left| \frac{\partial f}{\partial z} \right|^2 \right) c_i^2(\omega_\lambda) dz = \frac{l}{V} \quad (17)$$

where V is the volume of the superlattice. If the total ionic displacement is written in terms of the normal modes as

$$\mathbf{W}(\mathbf{r}) = \sum_\lambda \left(\frac{\hbar}{2\omega_\lambda \rho_{r_i}} \right)^{1/2} (a_{-\lambda}^\dagger + a_\lambda) \mathbf{W}_\lambda(\mathbf{r}) \quad (18)$$

thus

$$V(\mathbf{r}) = \sum_\lambda \left(\frac{\hbar}{2\omega_\lambda \rho_{r_i}} \right)^{1/2} (a_{-\lambda}^\dagger + a_\lambda) f(z) \exp(q_\parallel \cdot x_\parallel) \quad (19)$$

for guided modes A_G in (6) is given by (17). For interface modes A_I , B_I , C_I and D_I are obtained by the equations expressing the electrostatic boundary conditions (20) and (17):

$$\begin{aligned} A_I \exp(-q_\parallel a) + B_I \exp(q_\parallel a) &= C_I \exp(-q_\parallel a) + D_I \exp(q_\parallel a) \\ A_I \exp(q_\parallel a) + B_I \exp(-q_\parallel a) &= \{C_I \exp[q_\parallel(a-l)] \\ &\quad + D_I \exp[-q_\parallel(a-l)]\} \exp(iQl) \\ \kappa_1(\omega_\lambda)(A_I \exp(-q_\parallel a) - B_I \exp(q_\parallel a)) &= \kappa_2(\omega_\lambda)(C_I \exp(-q_\parallel a) - D_I \exp(q_\parallel a)) \\ \kappa_1(\omega_\lambda)(A_I \exp(q_\parallel a) - B_I \exp(-q_\parallel a)) &= \kappa_2(\omega_\lambda)\{C_I \exp[q_\parallel(a-l)] \\ &\quad - D_I \exp[-q_\parallel(a-l)]\} \exp(iQl). \end{aligned} \quad (20)$$

Non-trivial solutions of (20) are obtained when the following dispersion equation is satisfied:

$$\begin{aligned} \frac{1}{2} \left(\frac{\kappa_1(\omega_\lambda)}{\kappa_2(\omega_\lambda)} + \frac{\kappa_2(\omega_\lambda)}{\kappa_1(\omega_\lambda)} \right) \sinh(2q_\parallel b) \sinh(2q_\parallel a) \\ + \cosh(2q_\parallel b) \cosh(2q_\parallel a) = \cos(Ql). \end{aligned} \quad (21)$$

Here the dielectric constant in material i is given by

$$\kappa_i(\omega_\lambda) = \kappa_{\infty_i} + (\kappa_{0_i} - \kappa_{\infty_i}) [1 - (\omega_\lambda / \omega_{\text{TO}_i})^2]^{-1}. \quad (22)$$

The electron–optical phonon coupling term H_{ep} in the Hamiltonian is given by $H_{\text{ep}} = -eV$ and the scattering rate derived from Fermi's golden rule is

$$T(\mathbf{k}, n_\lambda | \mathbf{k}' n'_\lambda) = (2\pi/\hbar) |\langle \mathbf{k}', n'_\lambda | H_{\text{ep}} | \mathbf{k}, n_\lambda \rangle|^2 \delta[\varepsilon_{\mathbf{k}'} - \varepsilon_{\mathbf{k}} + (n'_\lambda - n_\lambda) \hbar \omega_\lambda]. \quad (23)$$

Simplification of (23) gives

$$T(\mathbf{k}, \mathbf{k}') = \frac{2\pi}{\hbar} \frac{e^2 \hbar}{2\omega_\lambda} (n_\lambda + \frac{1}{2} \pm \frac{1}{2}) |\langle \mathbf{k}' | \frac{f(z)}{\rho_{r_i}^{1/2}} \exp(iq_\parallel \cdot x_\parallel) | \mathbf{k} \rangle|^2 \delta(\varepsilon_{\mathbf{k}'} - \varepsilon_{\mathbf{k}} \pm \hbar \omega_\lambda). \quad (24)$$

Finally, by making use of (3) and taking $\phi(z)$ to be significant only when $|z| < l/2$ we obtain

$$T(\mathbf{k}, \mathbf{k}') = \frac{\pi e^2}{\omega_\lambda} (n_\lambda + \frac{1}{2} \pm \frac{1}{2}) \delta_{\mathbf{k}'_{\parallel} - \mathbf{k}_{\parallel}, \mathbf{q}_{\parallel}} \delta_{k'_z - k_z, Q} \left| \int_{-l/2}^{+l/2} \phi^2(z) f(z) \rho_{r_i}^{-1/2} dz \right|^2 \times \delta(\varepsilon_{\mathbf{k}'} - \varepsilon_{\mathbf{k}} \pm \hbar\omega_\lambda). \quad (25)$$

References

- [1] Riddoch F and Ridley B K 1985 *Physica B* **134** 342
- [2] Sawaki N 1986 *J. Phys. C: Solid State Phys.* **19** 4965
- [3] Wendler L, Haupt R, Bechstedt F, Rucker H and Enderlein R 1988 *Superlatt. Microstruct.* **4** 577
- [4] Ridley B K 1989 *Phys. Rev. B* **39** 5282
- [5] Palmier J and Chomette A 1982 *J. Physique* **43** 381
- [6] Warren G and Butcher P N 1986 *Semicond. Sci. Technol.* **1** 133
- [7] Devaud B, Shah J, Damen T C, Lambert B and Regreny A 1987 *Phys. Rev. Lett.* **58** 2582
- [8] Sibille A, Palmier J and Minot C 1989 *Appl. Phys. Lett.* **54** 165
- [9] Klein M V 1986 *IEEE J. Quantum Electron.* **QE-22** 1760
- [10] Cardona M 1989 *Superlatt. Microstruct.* **5** 27
- [11] Sawaki N and Akasaki I 1985 *Physica B* **134** 494
- [12] Barker A, Merz J and Gossard A C 1978 *Phys. Rev. B* **17** 3181
- [13] Fasolino A, Molinari E and Maan J C 1986 *Phys. Rev. B* **33** 8889
- [14] Babiker M 1987 *Physica B* **145** 111; 1986 *J. Phys. C: Solid State Phys.* **19** 683
- [15] Jusserand B and Paquet D 1985 *Superlatt. Microstruct.* **1** 61
- [16] Enderlein R, Beschstedt F and Gerecke G 1988 *Phys. Status Solidi b* **148** 173
- [17] Camley R E and Mills D L 1984 *Phys. Rev. B* **29** 1695
- [18] Fuchs R and Kliewer K 1965 *Phys. Rev.* **104** A2076
- [19] Ren S, Chu H and Change Y C 1988 *Phys. Rev. B* **37** 8899
- [20] Tsuchiya T, Akera H and Ando T 1989 *Phys. Rev. B* **39** 6025
- [21] Haug K and Zhu B F 1988 *Phys. Rev. B* **38** 2183, 12277
- [22] Zhu B F 1988 *Phys. Rev. B* **38** 7694
- [23] Fasolino A, Molinari E and Maan J C 1989 *Phys. Rev. B* **39** 3923
- [24] Richter E, Strauch D 1987 *Solid State Commun.* **64** 867
- [25] Born M and Huang K 1954 *Dynamical Theory of Crystal Lattices* (Oxford: OUP)
- [26] Haken H 1976 *Quantum Field Theory of Solids* (Amsterdam: North-Holland)
- [27] Bruesch P 1982 *Phonons: Theory and Experiment* vol 1 (Berlin: Springer)
- [28] Okumura H, Misawa S, Yoshida S and Gonda S 1985 *Appl. Phys. Lett.* **46** 4377
- [29] Sakaki H, Noda T, Hirakawa K, Tanaka M and Matsusue T 1987 *Appl. Phys. Lett.* **51** 1934